

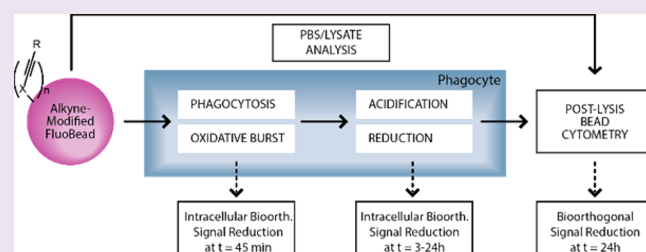
# Quantification of Bioorthogonal Stability in Immune Phagocytes Using Flow Cytometry Reveals Rapid Degradation of Strained Alkynes

Thomas Bakkum, Tyrza van Leeuwen, Alexi J. C. Sarris, Daphne M. van Elsland, Dimitrios Poulcharidis, Herman S. Overkleeft, and Sander I. van Kasteren\*

Leiden Institute of Chemistry and The Institute for Chemical Immunology, Leiden University, Einsteinweg 55, 2333 CC Leiden, The Netherlands

## Supporting Information

**ABSTRACT:** One of the areas in which bioorthogonal chemistry—chemistry performed inside a cell or organism—has become of pivotal importance is in the study of host–pathogen interactions. The incorporation of bioorthogonal groups into the cell wall or proteome of intracellular pathogens has allowed study within the endolysosomal system. However, for the approach to be successful, the incorporated bioorthogonal groups must be stable to chemical conditions found within these organelles, which are some of the harshest found in metazoans: the groups are exposed to oxidizing species, acidic conditions, and reactive thiols. Here we present an assay that allows the assessment of the stability of bioorthogonal groups within host cell phagosomes. Using a flow cytometry-based assay, we have quantified the relative label stability inside dendritic cell phagosomes of strained and unstrained alkynes. We show that groups that were shown to be stable in other systems were degraded by as much as 79% after maturation of the phagosome.



Bioorthogonal chemistry is the execution of a selective chemical reaction within the complex composition of a biological system.<sup>1</sup> It is often used for ligation purposes, whereby a small abiotic chemical functionality is first introduced into a biomolecule (or class of biomolecules) through metabolic engineering.<sup>2</sup> This chemical group is subsequently modified with a large detectable/retrievable group to realize its detection. Bioorthogonal ligation approaches have been used extensively, for example, to study the *in cellula*<sup>3,4</sup> and *in vivo*<sup>5</sup> dynamics of glycans, lipids,<sup>6</sup> nucleic acids,<sup>7,8</sup> prokaryotic<sup>9</sup> and eukaryotic proteomes,<sup>10</sup> and peptidoglycan.<sup>11</sup> The latter was used to label intracellular pathogens inside a phagocytic host cell to visualize this interaction.<sup>12</sup> The fact that bioorthogonal groups can be incorporated within amino acid side chains has even allowed us to visualize these pathogens as they are being degraded by the lysosomal hydrolases in macrophages and dendritic cells (DCs).<sup>13–16</sup> However, to provide unbiased results, their stability to intracellular conditions is essential to preventing label loss during the biological time course.

The antigen presenting cells (APCs) used in the above studies expose their phagosomal content to some of the harshest chemistries found in the body (Figure 1A).<sup>17,18</sup> When an APC phagocytoses a bacterium, the activity of the NADPH oxidase-2 complex (NOX2) will first result in the intraphagosomal generation of superoxide radicals ( $O_2^{\cdot-}$ ) to concentrations of 25–100  $\mu M$ <sup>19</sup> (in the absence of myelin peroxidase). This will rapidly be converted to hydrogen peroxide (<30  $\mu M$ )<sup>19</sup> but also

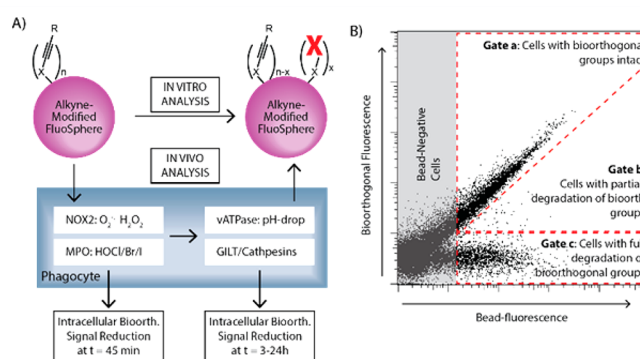


**Figure 1.** Outline of the stability assays and FACS analysis. (A) Alkyne-modified fluorescent latex beads were incubated either *in vitro* or fed to APCs and the reduction in the number of reactive alkynes assessed either of the naked beads or of the cells containing the beads. X depicts alkynes rendered unreactive. (B) Degradation in cells was quantified by counting the number of cells in which all bioorthogonal groups were degraded. The reason for this is that it allows objective gating for positive and negative cells. Bead fluorescence was used as an internal standard to negate differences in bead uptake between cells.

Received: April 18, 2018  
Accepted: April 25, 2018  
Published: April 25, 2018

NO radicals ( $<15 \mu\text{M}$ )<sup>20</sup> and hydroxyl radicals ( $\cdot\text{OH}$ ).<sup>21</sup> Myeloperoxidase can further convert these species to hypohalous acids, from the reaction between hydrogen peroxide and chloride anions.<sup>22,23</sup> This oxidative burst in APCs is followed by acidification of the vesicle down to pH values as low as 4.8 through the action of the vATPase proton pump.<sup>24</sup> During this process, the phagosome fuses with a lysosome containing a wide range of highly proteolytic and reducing enzymes and other hydrolases,<sup>25</sup> as well as the thioreductase GILT.<sup>26</sup>

This sequence of events renders traditional genetic labeling approaches of partial use as they will be degraded by the lysosomal proteases and thus rendered invisible. Even small molecule fluorophores are precluded due to their sensitivity to oxidation.<sup>27</sup>

Copper-catalyzed and strain-promoted Huisgen-type cycloaddition reactions (ccHc and spHc respectively) are among the most widely applied reactions for the study of intraphagosomal events.<sup>11,12,28,29</sup> However, the stability of the reaction partners in this environment has not previously been characterized, as it has, for example, been reported that alkynes are sensitive to thiols and/or radical conditions,<sup>30–33</sup> found in these organelles.<sup>34</sup> Yet, despite this potential stability risk, most stability studies of bioorthogonal groups have been performed in either buffered growth media or cell lysates,<sup>33</sup> or the cytosol of intact target cells.<sup>35,36</sup> None of these conditions recapitulate the chemical harshness of the maturing phagosome.

Here, we describe a method to quantify the bioorthogonal label stability inside phagosomes. Using an approach based on fluorescent beads modified with strained and unstrained alkynes, we have quantified their stability against the chemistries encountered during phagosomal maturation. Using this assay, we have found that strained alkynes are rapidly degraded under these conditions. Terminal alkynes on the other hand remain stable to the conditions found during the entire phagosomal maturation pathway. Subsequent *in vitro* analysis revealed the reaction between the spHc reagents, and sodium hypochlorite was a likely culprit for the sequestration of the bioorthogonal groups.

## RESULTS AND DISCUSSION

**Development of a Bioorthogonal Stability Assay in Phagocytes.** There are three main classes of phagocyte in the immune system, macrophages, dendritic cells (DCs), and neutrophils, of which dendritic cells and macrophages are both important for antigen processing and presentation. They are also the main reservoir for intracellular pathogenic bacteria and thus under intense scrutiny to study the host–bacterial pathogen interactions. DCs and macrophages—as well as their subsets—display wide heterogeneity regarding their phagocytic capacity and intracellular chemistries.<sup>37,38</sup> In order to develop an assay that would allow the assessment of the stability of bioorthogonal groups after phagocytosis independent of the differences in uptake, we designed an approach where we would let the phagocytes take up microspheres that not only were surface modified with the bioorthogonal groups but also contained intrabead fluorophores not exposed to the phagosomal environment (Figure 1a), thus showing minimal bleaching.<sup>39</sup> These beads would allow the quantification of bioorthogonal handles per bead over time inside a phagocyte, by measuring the change in ratio of fluorescent signal resulting from a bioorthogonal ligation to that of the internal fluorophore. This approach would negate not only differences

in uptake between cells but also signal changes resulting from any potential expulsion of beads through exocytosis<sup>37</sup> (Figure 1B). The approach is also facile, as the whole analysis could also be performed in fixed cells, preventing the need for reisolating the spheres after the biological time course.

We therefore modified amine-functionalized 0.2  $\mu\text{m}$  polystyrene FluoSpheres (excitation–emission: 580–605 nm, 5) with various bioorthogonal ligands for the azide–alkyne [3 + 2] cycloaddition (Figure 2) using hydroxysuccinimidyl (1–4)-

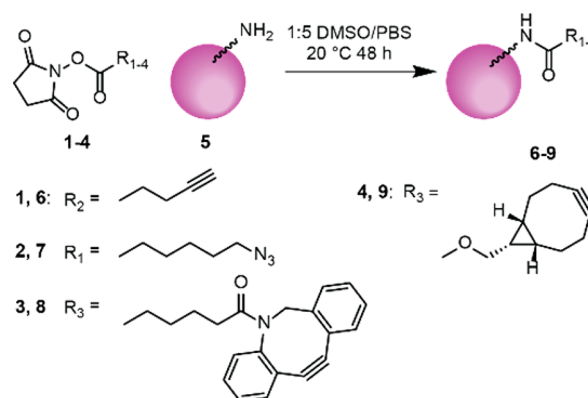


**Figure 2.** Synthesis of bioorthogonal fluorescent polystyrene beads. Amine-functionalized FluoSpheres 5 (200 nm) were modified with hydroxysuccinimidyl esters 1–4 to yield bioorthogonal FluoSpheres 6–9.

mediated amide/carbamate condensation reactions.<sup>40</sup> The acetylenyl and azido groups were chosen for their widespread application in the copper-catalyzed<sup>41</sup> or strain-promoted Huisgen cycloaddition<sup>42</sup> or the Bertozzi–Staudinger ligation.<sup>3</sup> The dibenzocyclooctynyl (DBCO, 3) and bicyclo[6.1.0]nonyne (BCN, 4) were chosen due to their rapid reported reaction rates ( $2.3 \text{ M}^{-1} \text{ s}^{-1}$  and  $0.3 \text{ M}^{-1} \text{ s}^{-1}$  respectively).<sup>43,44</sup> Optimal reaction conditions were found to be shaking the unmodified beads for 2 days at 20 °C in a 1:5 mixture of DMSO in PBS, containing a large excess of the succinimidyl esters 1–4 to yield acetylenyl- (6), azido- (7), dibenzocyclooctynyl (8), or bicyclo[6.1.0]nonyne (9)-modified FluoSpheres.

The fluorescence of the beads allowed their assessment by bead-only flow cytometry: using either a copper-catalyzed or copper-free [3 + 2] cycloaddition reaction (in the case of 6 and 7) with AF488-azide/alkyne,<sup>8,45</sup> followed by flow cytometric analysis of the FluoSpheres (Figure 3,  $t = 0$ ) to visualize the introduced alkynes or fluorescamine to visualize the remaining unreacted amines (Figure S1).<sup>46</sup> Complete disappearance of the fluorescamine signal was observed for all particles, indicating complete consumption of the free amine functionalities in all reactions.

**Stability of Bioorthogonal FluoSpheres *in Vitro*.** We first determined whether this assay could recapitulate previously reported stability observations of the various above bioorthogonal groups (Figure 3, Figures S2–S7).<sup>35</sup> All groups were previously reported to be stable in PBS and cell lysates, but strained alkynes were reported to react with thiols<sup>30,47</sup> and thiol radicals.<sup>30</sup> Alkynes were shown also to be reactive toward thiol radicals in this same study, as well as to hydroxyl radicals.<sup>48,49</sup>

The bioorthogonal FluoSpheres were first incubated (in triplicate) in DC2.4<sup>50</sup> cell lysate (Figure S3) or PBS (Figure S4) for up to 24 h and subsequently reacted with AF488-azide

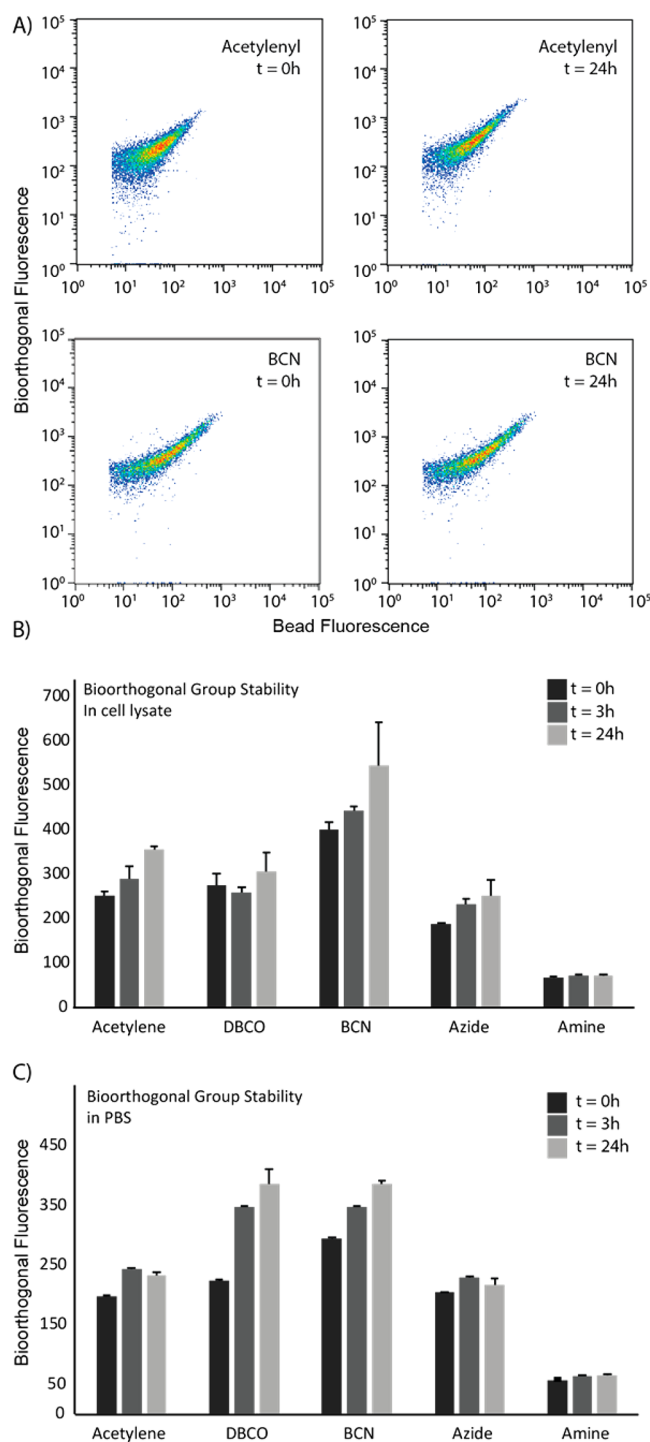


**Figure 3.** Assessment of stability of bioorthogonal groups in cell lysate or PBS. (A) Plots at  $t = 0$  and  $t = 24$  of an incubation of acetylenyl-FluoSpheres 5 and BCN-FluoSpheres 9 in cell lysate. The y axis shows the fluorescence stemming from bioorthogonal ligations; the x axis, the intrinsic fluorescence of the spheres. (B) Quantification of the median bioorthogonal fluorescence over time of the modified FluoSpheres 5–9 in cell lysate and (C) in PBS (see also Figures S2–S4).

(or alkyne in case of azide) using the appropriate bioorthogonal ligation conditions (Figures 3, S2). The beads were then injected directly into the flow cytometer for quantification of both the bead-based and bioorthogonal-based fluorescent signal. The internal fluorescent dye could readily be used to discriminate beads from cellular debris of a similar size.

Changes in the median fluorescence of the bioorthogonally introduced fluorophore allowed quantification of the remaining signal. None of the bioorthogonal groups showed significant reduction in lysate (Figures 3B, S2, S3) and PBS (Figures 3C, S2, S4). An increase in signal over time was even observed, possibly due to deaggregation of the beads in these media. When assessing whether the thiol and thiol reactivity could be recapitulated, it was indeed found that all groups completely degraded, as expected in the presence of 250 mM glutathione (GSH) and the radical initiator 2-hydroxy-4'-(2-hydroxyethoxy)-2-methylpropiophenone (25 mM) after 5 or 10 min of irradiation with UV light ( $145 \mu\text{W}/\text{cm}^2$ ) to generate radicals *in situ* (Figures S2 and S5). Even without radicals, all bioorthogonal signals disappeared after incubation with GSH for 30 min (Figures S2 and S6). Radicals alone resulted in the exclusive degradation of BCN and DBCO (Figures S2 and S7), confirming the suitability of this approach at least *in vitro*.

**Stability of Bioorthogonal FluoSpheres in Cells.** We next tested the stability of bioorthogonal FluoSpheres 6–9 in the endolysosomal environment of phagocytes. We employed the DC2.4 cell line as our source of DC<sup>50</sup> and RAW264.7 cells as a macrophage cell line,<sup>51</sup> as they lie at either end of the property spectrum of phagocytes: DC2.4s phagocytose in a controlled manner and use their oxidative burst to attenuate protease activity, leading to improved antigen presentation, either by oxidizing cysteine proteases and reducing the reductive capacity of the phagosome<sup>52</sup> or by limiting the acidification of the phagosome.<sup>53,54</sup> RAW264.7s are macrophage-like and have a very high phagocytic capacity.<sup>55</sup> They are also capable of producing reactive oxygen species in high amounts,<sup>56</sup> as well as secondary ROS metabolites through the action of myeloperoxidase (MPO).<sup>57</sup>

The assay was designed as follows: RAW264.7 cells were first allowed to take up the bioorthogonal FluoSpheres for 45 min ( $t = 0$ ), after which uptake and the initial oxidative burst would be complete.<sup>58</sup> Due to their size, the particles remain within the confines of the phago-lysosomal system.<sup>59</sup> The cells were then washed and chased for 3 or 24 h to determine to what extent acidification, thioreductase expression,<sup>26</sup> and proteolysis<sup>60,61</sup> in the matured phagosome contributed to bioorthogonal handle degradation. Cells were then fixed and permeabilized (allowing free entry of bioorthogonal reagents and neutralization of the phagosomal compartment), ligated with a complementary bioorthogonal fluorophore, before quantification of the two fluorescent signals by flow cytometry (Figure 4, Figures S8 and S9). Fluorescence in the red channel (FluoSpheres) was plotted against green fluorescence (AF488 coupled to the bioorthogonal groups) after excluding dead cells and debris. Quantification gates were set to exclude cells and debris that had not taken up beads (Figures 1B and 4A, gray area). Bioorthogonal degradation was quantified (Figure 4A) by looking at the percentage of cells in which the bioorthogonal fluorescence had been reduced to the level of unmodified FluoSpheres 5. DC2.4 cells were used as a more dendritic cell-like antigen presenting cell line.<sup>50</sup>

The acetylenyl groups on FluoSpheres 6 showed a remarkable stability in both DC2.4s and RAW264.7 cells (Figure 4A/B, Figures S8 and S9) with <6% degradation observed at any time point in either RAW264.7s or DC2.4s. BCN groups showed the lowest stability, especially to the intracellular conditions found in RAW264.7 cells:  $79\% \pm 1.8\%$  of cells had fully degraded all bioorthogonal groups after 24 h. DBCO groups showed a moderate stability ( $36\% \pm 0.8\%$



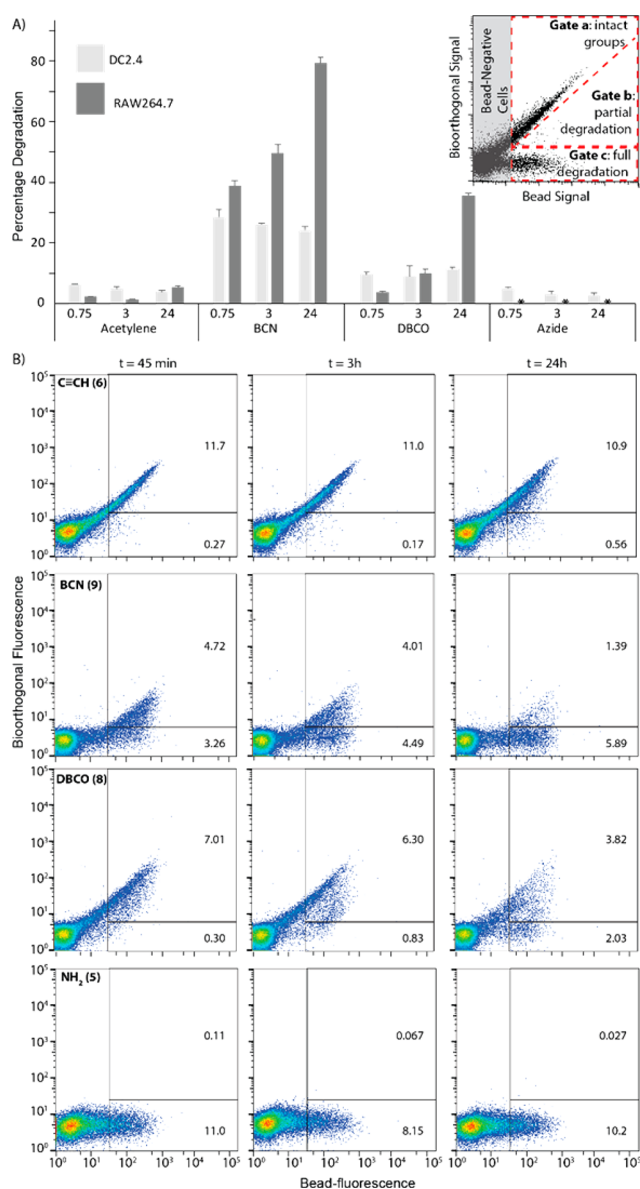


**Figure 4.** Quantification of bioorthogonal group stability. (A) Percentage of degraded bioorthogonal groups after incubation in DC2.4 or RAW 264.7 cells, as quantified by illustrated gating strategy (insert and Figure 1B). Cells that had not taken up beads (gray area) were excluded from the gated area; cells in which the bioorthogonal signal had fully degraded to background (gate B) were counted, as were the cells still positive for bioorthogonal signal (gate A). (B) Quantification of percentage RAW 264.7 cells containing degraded beads ( $B/[A + B]$ ) (see also Figure S9). Indicated values are fractions of total cell count.

degradation after 24 h). Azide-modified spheres showed very poor uptake in RAW264.7 cells, preventing the quantification of their degradation in these cells. In DC2.4 cells, degradation was, however, minimal (Figure 4A and Figures S8 and S9). Attempts to further enhance degradation by stimulating the oxidative burst by adding phorbol-12-myristoyl-13-acetate (PMA) and yeast-derived zymosan particles to both cell lines<sup>62</sup> did not yield a further increase in degradation (Figures S10 and S11). In fact, the dual addition of particles and these stimuli resulted in extensive cell death over the time course of the experiment, again preventing quantification of the degradation.

We were intrigued by the degradation shown only for strained alkynes and not the acetylene and azide groups. We postulated that this was likely due to radicals present during phagosomal maturation, as extensive degradation was already observed at the earliest time point. We hypothesized that the potential culprits could be superoxide, the superoxide metabolite  $H_2O_2$ , which can reach on the order of  $100 \mu M$  if MPO is inhibited,<sup>63</sup> or the species produced by myeloperoxidase, such as hypochlorous acid. This species is produced by MPO in the presence of imported chlorine and can reach high micromolar concentrations in the phagosome.<sup>18,64</sup> It is also the reagent that sparked the development of the addition rules by Markovnikov in its ability to add across a triple bond.<sup>65</sup> One unresolved issue in this hypothesis is that HOCl production is well established in neutrophils, but less is known about its intracellular concentrations in DCs and macrophages, due to the interplay between MPO and chloride channels in these cells.<sup>64,66–68</sup> Other potential reaction partners could be hydroxyl radicals produced through Fenton chemistry or thiol oxidation products produced during the oxidative burst.<sup>19</sup>

To determine the responsible species, we returned to the *in vitro* system to assess whether the reactive species in the endosome could degrade bioorthogonal handles at the concentrations found in the phagosome. Compounds 6–9 were incubated with hydrogen peroxide concentrations of 50, 100, or  $200 \mu M$  at pH 7.4 or 5.0, either in the dark (Figure S12) or while exposed to UV radiation ( $145 \mu W/cm^2$  for 5 min, Figure S13). All particles proved stable under these conditions, suggesting the primary products of oxidative burst are not responsible for the in-cell degradation. Incubation with the MPO product sodium hypochlorite at the same concentrations and again at either pH 7.4 or 5.0 did show the same stability pattern as observed in both RAW264.7 and DC2.4 cells: 8 and 9 were degraded under these conditions, whereas 5 and 6 remained stable (Figure S14). Surprisingly, the degradation of BCN and DBCO only occurred at neutral pH and not the expected acidic pH. A reaction of the bioorthogonal Fluorospheres with GSH ( $100 \mu M$  or 1 mM) in the presence of *in-situ*-generated radicals was also performed to assess the potential role of thiols and thiol radicals in the degradation of the beads. Surprisingly, the strained alkynes proved stable to these conditions, whereas the acetylene and azide were degraded under acidic incubation with GSH and radicals (Figure S15). This makes the thiol-radical species an unlikely degradation candidate *in cellula*. The likely mechanism of degradation is probably a combination of the above factors, or a set of conditions as yet undescribed.

Using our simple bead-based assay to test the stability of bioorthogonal handles within the endolysosomal compartments of dendritic cells, we observed a striking difference in the disappearance of the reactivity of different bioorthogonal alkynes in phagocytes. These are obviously not the only class of bioorthogonal reactions used. Many other bioorthogonal ligation reactions are available,<sup>69</sup> such as the inverse electron-demand Diels–Alder cycloaddition,<sup>70,71</sup> the [4 + 1] photoclick,<sup>72</sup> diazo-based ligation reactions,<sup>73</sup> and many more.<sup>69</sup> Most of these have been incompletely profiled with regard to their *in cellula* stability, and we thus foresee that this simple assay could also provide insight also into the biostability of these groups and those yet to be discovered.

**■ ASSOCIATED CONTENT****Supporting Information**

The Supporting Information is available free of charge on the ACS Publications website at DOI: 10.1021/acschembio.8b00355.

Figures, raw cytometry plots, and experimental details (PDF)

**■ AUTHOR INFORMATION****Corresponding Author**

\*E-mail: s.i.van.kasteren@chem.leidenuniv.nl.

**ORCID**

Sander I. van Kasteren: 0000-0003-3733-818X

**Author Contributions**

All authors have given approval to the final version of the manuscript.

**Funding**

T.B. and S.I.v.K. were funded by The Netherlands Council for Scientific Research (NWO). A.J.C.S., H.S.O., and S.I.v.K. were funded by the Institute for Chemical Immunology Zwaartekracht program (ICI). S.I.v.K. was funded by the European Research Council (ERC grant no: 639005).

**Notes**

The authors declare no competing financial interest.

**■ ACKNOWLEDGMENTS**

We would like to thank K. Rock (UMass Medical School) for providing us with the DC2.4 cell line.

**■ ABBREVIATIONS**

APC, antigen presenting cell; DC, dendritic cell

**■ REFERENCES**

- (1) Sletten, E. M., and Bertozzi, C. R. (2009) Bioorthogonal chemistry: fishing for selectivity in a sea of functionality. *Angew. Chem., Int. Ed.* 48, 6974–98.
- (2) McKay, C. S., and Finn, M. G. (2014) Click Chemistry in Complex Mixtures: Bioorthogonal Bioconjugation. *Chem. Biol.* 21, 1075–1101.
- (3) Saxon, E., and Bertozzi, C. R. (2000) Cell surface engineering by a modified Staudinger reaction. *Science* 287, 2007–2010.
- (4) Yarema, K. J., Mahal, L. K., Bruehl, R. E., Rodriguez, E. C., and Bertozzi, C. R. (1998) Metabolic delivery of ketone groups to sialic acid residues. Application To cell surface glycoform engineering. *J. Biol. Chem.* 273, 31168–79.
- (5) Laughlin, S. T., Baskin, J. M., Amacher, S. L., and Bertozzi, C. R. (2008) In vivo imaging of membrane-associated glycans in developing zebrafish. *Science* 320, 664–667.
- (6) Hang, H. C., Wilson, J. P., and Charron, G. (2011) Bioorthogonal chemical reporters for analyzing protein lipidation and lipid trafficking. *Acc. Chem. Res.* 44, 699–708.
- (7) Jao, C. Y., and Salic, A. (2008) Exploring RNA transcription and turnover in vivo by using click chemistry. *Proc. Natl. Acad. Sci. U. S. A.* 105, 15779–84.
- (8) Salic, A., and Mitchison, T. J. (2008) A chemical method for fast and sensitive detection of DNA synthesis in vivo. *Proc. Natl. Acad. Sci. U. S. A.* 105, 2415–2420.
- (9) Van Hest, J. C. M., Kiick, K. L., and Tirrell, D. A. (2000) Efficient incorporation of unsaturated methionine analogues into proteins in vivo. *J. Am. Chem. Soc.* 122, 1282–1288.
- (10) Dieterich, D. C., Link, A. J., Graumann, J., Tirrell, D. A., and Schuman, E. M. (2006) Selective identification of newly synthesized proteins in mammalian cells using bioorthogonal noncanonical amino

acid tagging (BONCAT). *Proc. Natl. Acad. Sci. U. S. A.* 103, 9482–9487.

- (11) Siegrist, M. S., Whiteside, S., Jewett, J. C., Aditham, A., Cava, F., and Bertozzi, C. R. (2013) d-Amino Acid Chemical Reporters Reveal Peptidoglycan Dynamics of an Intracellular Pathogen. *ACS Chem. Biol.* 8, 500–505.

- (12) Siegrist, M. S., Aditham, A. K., Espallat, A., Cameron, T. A., Whiteside, S. A., Cava, F., Portnoy, D. A., and Bertozzi, C. R. (2015) Host actin polymerization tunes the cell division cycle of an intracellular pathogen. *Cell Rep.* 11, 499–507.

- (13) van Elsland, D. M., Bos, E., de Boer, W., Overkleeft, H. S., Koster, A. J., and van Kasteren, S. I. (2016) Detection of bioorthogonal groups by correlative light and electron microscopy allows imaging of degraded bacteria in phagocytes. *Chem. Sci.* 7, 752–758.

- (14) van Elsland, D. M., and van Kasteren, S. I. (2016) Imaging Bioorthogonal Groups in Their Ultrastructural Context with Electron Microscopy. *Angew. Chem., Int. Ed.* 55, 9472–9473.

- (15) Pawlak, J. B., Hos, B. J., van de Graaff, M. J., Megantari, O. A., Meeuwenoord, N., Overkleeft, H. S., Filippov, D. V., Ossendorp, F., and van Kasteren, S. I. (2016) The Optimization of Bioorthogonal Epitope Ligation within MHC-I Complexes. *ACS Chem. Biol.* 11, 3172–3178.

- (16) Pawlak, J. B., Gential, G. P., Ruckwardt, T. J., Bremmers, J. S., Meeuwenoord, N. J., Ossendorp, F. A., Overkleeft, H. S., Filippov, D. V., and van Kasteren, S. I. (2015) Bioorthogonal Deprotection on the Dendritic Cell Surface for Chemical Control of Antigen Cross-Presentation. *Angew. Chem., Int. Ed.* 54, 5628–5631.

- (17) Flannagan, R. S., Cosio, G., and Grinstein, S. (2009) Antimicrobial mechanisms of phagocytes and bacterial evasion strategies. *Nat. Rev. Microbiol.* 7, 355–66.

- (18) Fang, F. C. (2011) Antimicrobial Actions of Reactive Oxygen Species. *mBio* 2, e00141-11.

- (19) Winterbourn, C. C., Hampton, M. B., Livesey, J. H., and Kettle, A. J. (2006) Modeling the Reactions of Superoxide and Myeloperoxidase in the Neutrophil Phagosome: Implications for Microbial Killing. *J. Biol. Chem.* 281, 39860–39869.

- (20) Xiong, Q., Tezuka, Y., Kaneko, T., Li, H., Tran, L. Q., Hase, K., Namba, T., and Kadota, S. (2000) Inhibition of nitric oxide by phenylethanoids in activated macrophages. *Eur. J. Pharmacol.* 400, 137–144.

- (21) Slauch, J. M. (2011) How does the oxidative burst of macrophages kill bacteria? Still an open question. *Mol. Microbiol.* 80, 580–583.

- (22) Furtmuller, P. G., Obinger, C., Hsuanyu, Y., and Dunford, H. B. (2000) Mechanism of reaction of myeloperoxidase with hydrogen peroxide and chloride ion. *Eur. J. Biochem.* 267, 5858–64.

- (23) Klebanoff, S. J., Kettle, A. J., Rosen, H., Winterbourn, C. C., and Nauseef, W. M. (2013) Myeloperoxidase: a front-line defender against phagocytosed microorganisms. *J. Leukocyte Biol.* 93, 185–198.

- (24) Ohkuma, S., and Poole, B. (1978) Fluorescence probe measurement of the intralysosomal pH in living cells and the perturbation of pH by various agents. *Proc. Natl. Acad. Sci. U. S. A.* 75, 3327–3331.

- (25) Turk, V., Stoka, V., Vasiljeva, O., Renko, M., Sun, T., Turk, B., and Turk, D. (2012) Cysteine cathepsins: From structure, function and regulation to new frontiers. *Biochim. Biophys. Acta, Proteins Proteomics* 1824, 68–88.

- (26) Arunachalam, B., Phan, U. T., Geuze, H. J., and Cresswell, P. (2000) Enzymatic reduction of disulfide bonds in lysosomes: Characterization of a Gamma-interferon-inducible lysosomal thiol reductase (GILT). *Proc. Natl. Acad. Sci. U. S. A.* 97, 745–750.

- (27) Chen, Y., and Junger, W. G. (2012) Measurement of Oxidative Burst in Neutrophils. *Methods Mol. Biol.* 844, 115–124.

- (28) Shieh, P., Siegrist, M. S., Cullen, A. J., and Bertozzi, C. R. (2014) Imaging bacterial peptidoglycan with near-infrared fluorogenic azide probes. *Proc. Natl. Acad. Sci. U. S. A.* 111, 5456–5461.

- (29) Liechti, G. W., Kuru, E., Hall, E., Kalinda, A., Brun, Y. V., VanNieuwenhze, M., and Maurelli, A. T. (2014) A new metabolic cell-

wall labelling method reveals peptidoglycan in *Chlamydia trachomatis*. *Nature* 506, 507–510.

(30) Lo Conte, M., Staderini, S., Marra, A., Sanchez-Navarro, M., Davis, B. G., and Dondoni, A. (2011) Multi-molecule reaction of serum albumin can occur through thiol-yne coupling. *Chem. Commun.* 47, 11086–11088.

(31) Ekkebus, R., van Kasteren, S. I., Kulathu, Y., Scholten, A., Berlin, I., Geurink, P. P., de Jong, A., Goerdal, S., Neefjes, J., Heck, A. J. R., Komander, D., and Ova, H. (2013) On Terminal Alkynes That Can React with Active-Site Cysteine Nucleophiles in Proteases. *J. Am. Chem. Soc.* 135, 2867–2870.

(32) Sommer, S., Weikart, N. D., Linne, U., and Mootz, H. D. (2013) Covalent inhibition of SUMO and ubiquitin-specific cysteine proteases by an in situ thiol-alkyne addition. *Bioorg. Med. Chem.* 21, 2511–2517.

(33) Tian, H., Sakmar, T. P., and Huber, T. (2016) A simple method for enhancing the bioorthogonality of cyclooctyne reagent. *Chem. Commun.* 52, 5451–4.

(34) Jiang, X., Yu, Y., Chen, J., Zhao, M., Chen, H., Song, X., Matzuk, A. J., Carroll, S. L., Tan, X., Sizovs, A., Cheng, N., Wang, M. C., and Wang, J. (2015) Quantitative Imaging of Glutathione in Live Cells Using a Reversible Reaction-Based Ratiometric Fluorescent Probe. *ACS Chem. Biol.* 10, 864–874.

(35) Murrey, H. E., Judkins, J. C., am Ende, C. W., Ballard, T. E., Fang, Y., Riccardi, K., Di, L., Guilmette, E. R., Schwartz, J. W., Fox, J. M., and Johnson, D. S. (2015) Systematic Evaluation of Bioorthogonal Reactions in Live Cells with Clickable HaloTag Ligands: Implications for Intracellular Imaging. *J. Am. Chem. Soc.* 137, 11461–11475.

(36) Beatty, K. E., Fisk, J. D., Smart, B. P., Lu, Y. Y., Szychowski, J., Hangauer, M. J., Baskin, J. M., Bertozzi, C. R., and Tirrell, D. A. (2010) Live-cell imaging of cellular proteins by a strain-promoted azide-alkyne cycloaddition. *ChemBioChem* 11, 2092–5.

(37) Oh, N., and Park, J.-H. (2014) Endocytosis and exocytosis of nanoparticles in mammalian cells. *Int. J. Nanomed.* 9, 51–63.

(38) Helft, J., Bottcher, J., Chakravarty, P., Zelenay, S., Huotari, J., Schraml, B. U., Goubau, D., and Reis e Sousa, C. (2015) GM-CSF Mouse Bone Marrow Cultures Comprise a Heterogeneous Population of CD11c(+)MHCII(+) Macrophages and Dendritic Cells. *Immunity* 42, 1197–211.

(39) Steinkamp, J. A., Wilson, J. S., Saunders, G. C., and Stewart, C. C. (1982) Phagocytosis: flow cytometric quantitation with fluorescent microspheres. *Science* 215, 64–6.

(40) Borrmann, A., Milles, S., Plass, T., Dommerholt, J., Verkade, J. M., Wiessler, M., Schultz, C., van Hest, J. C., van Delft, F. L., and Lemke, E. A. (2012) Genetic encoding of a bicyclo[6.1.0]nonyne-charged amino acid enables fast cellular protein imaging by metal-free ligation. *ChemBioChem* 13, 2094–9.

(41) Meldal, M., and Tornøe, C. W. (2008) Cu-catalyzed azide - Alkyne cycloaddition. *Chem. Rev.* 108, 2952–3015.

(42) Agard, N. J., Prescher, J. A., and Bertozzi, C. R. (2004) A Strain-Promoted [3 + 2] Azide-Alkyne Cycloaddition for Covalent Modification of Biomolecules in Living Systems. *J. Am. Chem. Soc.* 126, 15046–15047.

(43) Ning, X., Guo, J., Wolfert, M. A., and Boons, G. J. (2008) Visualizing metabolically labeled glycoconjugates of living cells by copper-free and fast huisgen cycloadditions. *Angew. Chem., Int. Ed.* 47, 2253–5.

(44) Dommerholt, J., Schmidt, S., Temming, R., Hendriks, L. J., Rutjes, F. P., van Hest, J. C., Lefeber, D. J., Friedl, P., and van Delft, F. L. (2010) Readily accessible bicyclononynes for bioorthogonal labeling and three-dimensional imaging of living cells. *Angew. Chem., Int. Ed.* 49, 9422–5.

(45) Hong, V., Steinmetz, N. F., Manchester, M., and Finn, M. G. (2010) Labeling Live Cells by Copper-Catalyzed Alkyne–Azide Click Chemistry. *Bioconjugate Chem.* 21, 1912–1916.

(46) Udenfriend, S., Stein, S., Bohlen, P., Dairman, W., Leimgruber, W., and Weigele, M. (1972) Fluorescamine: a reagent for assay of amino acids, peptides, proteins, and primary amines in the picomole range. *Science* 178, 871–2.

(47) van Geel, R., Pruijn, G. J. M., van Delft, F. L., and Boelens, W. C. (2012) Preventing Thiol-Yne Addition Improves the Specificity of Strain-Promoted Azide-Alkyne Cycloaddition. *Bioconjugate Chem.* 23, 392–398.

(48) Lockhart, J., Blitz, M. A., Heard, D. E., Seakins, P. W., and Shannon, R. J. (2013) Mechanism of the Reaction of OH with Alkynes in the Presence of Oxygen. *J. Phys. Chem. A* 117, 5407–5418.

(49) Senosiain, J. P., Klippenstein, S. J., and Miller, J. A. (2005) The Reaction of Acetylene with Hydroxyl Radicals. *J. Phys. Chem. A* 109, 6045–6055.

(50) Shen, Z., Reznikoff, G., Dranoff, G., and Rock, K. L. (1997) Cloned dendritic cells can present exogenous antigens on both MHC class I and class II molecules. *J. Immunol.* 158, 2723–30.

(51) Ralph, P., and Nakoinz, I. (1977) Antibody-dependent killing of erythrocyte and tumor targets by macrophage-related cell lines: enhancement by PPD and LPS. *J. Immunol.* 119, 950–54.

(52) Rybicka, J. M., Balce, D. R., Chaudhuri, S., Allan, E. R. O., and Yates, R. M. (2012) Phagosomal proteolysis in dendritic cells is modulated by NADPH oxidase in a pH-independent manner. *EMBO J.* 31, 932–944.

(53) Savina, A., Peres, A., Cebrian, I., Carmo, N., Moita, C., Hacohen, N., Moita, L. F., and Amigorena, S. (2009) The small GTPase Rac2 controls phagosomal alkalization and antigen crosspresentation selectively in CD8(+) dendritic cells. *Immunity* 30, 544–55.

(54) Savina, A., Jancic, C., Hugues, S., Guermonprez, P., Vargas, P., Moura, I. C., Lennon-Duménil, A.-M., Seabra, M. C., Raposo, G., and Amigorena, S. (2006) NOX2 Controls Phagosomal pH to Regulate Antigen Processing during Crosspresentation by Dendritic Cells. *Cell* 126, 205–218.

(55) Kapellos, T. S., Taylor, L., Lee, H., Cowley, S. A., James, W. S., Iqbal, A. J., and Greaves, D. R. (2016) A novel real time imaging platform to quantify macrophage phagocytosis. *Biochem. Pharmacol.* 116, 107–119.

(56) Rybicka, J. M., Balce, D. R., Khan, M. F., Krohn, R. M., and Yates, R. M. (2010) NADPH oxidase activity controls phagosomal proteolysis in macrophages through modulation of the luminal redox environment of phagosomes. *Proc. Natl. Acad. Sci. U. S. A.* 107, 10496–10501.

(57) Adachi, Y., Kindzelskii, A. L., Petty, A. R., Huang, J.-B., Maeda, N., Yotsumoto, S., Aratani, Y., Ohno, N., and Petty, H. R. (2006) IFN- $\gamma$  Primes RAW264 Macrophages and Human Monocytes for Enhanced Oxidant Production in Response to CpG DNA via Metabolic Signaling: Roles of TLR9 and Myeloperoxidase Trafficking. *J. Immunol.* 176, 5033–5040.

(58) VanderVen, B. C., Yates, R. M., and Russell, D. G. (2009) Intraphagosomal measurement of the magnitude and duration of the oxidative burst. *Traffic* 10, 372–8.

(59) Claudia, M., Kristin, Ö., Jennifer, O., Eva, R., and Eleonore, F. (2017) Comparison of fluorescence-based methods to determine nanoparticle uptake by phagocytes and non-phagocytic cells in vitro. *Toxicology* 378, 25–36.

(60) van Kasteren, S. I., and Overkleeft, H. S. (2014) Endo-lysosomal proteases in antigen presentation. *Curr. Opin. Chem. Biol.* 23, 8–15.

(61) van Kasteren, S. I., Berlin, I., Colbert, J. D., Keane, D., Ova, H., and Watts, C. (2011) A Multifunctional Protease Inhibitor To Regulate Endolysosomal Function. *ACS Chem. Biol.* 6, 1198–1204.

(62) Mantegazza, A. R., Savina, A., Vermeulen, M., Pérez, L., Geffner, J., Hermine, O., Rosenzweig, S. D., Faure, F., and Amigorena, S. (2008) NADPH oxidase controls phagosomal pH and antigen cross-presentation in human dendritic cells. *Blood* 112, 4712–4722.

(63) Winterbourn, C. C., and Kettle, A. J. (2013) Redox reactions and microbial killing in the neutrophil phagosome. *Antioxid. Redox Signaling* 18, 642–60.

(64) Klebanoff, S. J. (2005) Myeloperoxidase: friend and foe. *J. Leukocyte Biol.* 77, 598–625.

(65) Markovnikov, V. (1870) Ueber die Abhängigkeit der verschiedenen Vertretbarkeit des Radicalwasserstoffs in den isomeren Buttersäure. *Liebigs Ann. Chem.* 153, 228–259.



(66) Scholz, W., Platzer, B., Schumich, A., Hocher, B., Fritsch, G., Knapp, W., and Strobl, H. (2004) Initial human myeloid/dendritic cell progenitors identified by absence of myeloperoxidase protein expression. *Exp. Hematol.* 32, 270–6.

(67) Pickl, W. F., Majdic, O., Kohl, P., Stöckl, J., Riedl, E., Scheinecker, C., Bello-Fernandez, C., and Knapp, W. (1996) Molecular and functional characteristics of dendritic cells generated from highly purified CD14+ peripheral blood monocytes. *J. Immunol.* 157, 3850–3859.

(68) Nunes, P., Demaurex, N., and Dinauer, M. C. (2013) Regulation of the NADPH Oxidase and Associated Ion Fluxes During Phagocytosis. *Traffic* 14 (11), 1118–1131.

(69) Lang, K., and Chin, J. W. (2014) Bioorthogonal reactions for labeling proteins. *ACS Chem. Biol.* 9, 16–20.

(70) Blackman, M. L., Royzen, M., and Fox, J. M. (2008) Tetrazine Ligation: Fast Bioconjugation Based on Inverse-Electron-Demand Diels–Alder Reactivity. *J. Am. Chem. Soc.* 130, 13518–13519.

(71) Oliveira, B. L., Guo, Z., and Bernardes, G. J. L. (2017) Inverse electron demand Diels–Alder reactions in chemical biology. *Chem. Soc. Rev.* 46, 4895–4950.

(72) Song, W., Wang, Y., Qu, J., and Lin, Q. (2008) Selective Functionalization of a Genetically Encoded Alkene-Containing Protein via “Photoclick Chemistry” in Bacterial Cells. *J. Am. Chem. Soc.* 130, 9654–9655.

(73) Andersen, K. A., Aronoff, M. R., McGrath, N. A., and Raines, R. T. (2015) Diazo Groups Endure Metabolism and Enable Chemo-selectivity in Cellulo. *J. Am. Chem. Soc.* 137, 2412–2415.